An Introduction to the Loewner Equation and SLE

David Duncan

1 Introduction

This paper is meant to serve as an introduction and reference guide to the Loewner equation and Stochastic Loewner Evolution (SLE). We begin by discussing various forms of Loewner's differential equation and some of the technical language of the surrounding mathematics. After proving the ability for the equation to generate slits in the upper-halfplane we investigate some properties and theorems that will be beneficial when we deal with SLE. Our attention is then turned to the realm of stochastic processes as we introduce Brownian motion and how it is used as a driving term to generate SLE. Since modeling SLE is (at the time of this publication) our primary endeavor, I have tried to use the mathematics developed in the previous sections to explain how this can be achieved both theoretically and in practice. Finally, we look at a specific example of a simple program that generates SLE for various values of κ. It is this program that serves as a base for modeling SLE via Mathematica. Although the more recent programs have made a number of developments, they all still use the same basic idea so it will be beneficial to understand how it works.

This paper was targeted toward those who have an understanding of real and complex analysis. However, an introduction to probability would also be beneficial. Beyond this I have tried to make it as self-contained as possible and have included two appendices to supplement some of the more specific background information.

2 Loewner equations

The heart of our focus is on the Loewner equation. This equation was studied extensively by Czech mathematician Charles Loewner. You may come across various spellings of his names including any combination of Karl, Karel, Charles for his first name and Löwner or Loewner for his last. He attended Charles University of Prague and received his Ph.D. in geometric function theory in 1917. In the years to follow he was employed at the German Technical University in Prague, the University of Berlin, the University of Cologne and the Charles University of Prague. In 1923 Loewner used the equation bearing his namesake to prove a special case of the

Bieberbach conjecture. The Loewner equation appeared again in de Branges' 1984 proof of the complete Bieberbach conjecture. Due to the Nazi influence in Germany, Loewner and his family were forced to emigrate to America where Loewner took a position at Louisville University. He finally moved on to Brown in 1944 where he worked on a program related to the war. [11]

There are a quite a few versions of Loewner's differential equation depending on which domain we are interested in. For example there are versions in the disk, the upper-halfplane, various annular domains and other even more obscure ones. Our primary focus is on the chordal Loewner equation, which is the Loewner equation in the upper half complex plane. However in some contexts it may be beneficial to use the radial Loewner equation, which takes the disk as its domain, so we will briefly discuss this as well.

2.1 Radial Loewner equation

As stated above, the radial Loewner equation generates a function that takes a subset of the disk to the whole disk. The equation has the form:

$$\frac{\partial}{\partial t}g(t,z) = -g(t,z)\frac{g(t,z)+\lambda(t)}{g(t,z)-\lambda(t)}, \qquad g(0,z)=z, \tag{1}$$

where $\lambda : [0,T] \to \mathbf{R}$ is a continuous function of t and $z \in \{z : |z| < 1\}$.

2.2 Chordal Loewner equation

There are two ways of looking at the chordal (half-plane) Loewner equation: i) by running time forwards and ii) by running time backwards. We investigate both below.

2.2.1 Forward Loewner equation

The forward version of the chordal Loewner equation is a differential equation having the form:

$$\frac{\partial}{\partial t}g(t,z) = \frac{2}{g(t,z)-\lambda(t)}, \qquad g(0,z)=z, \tag{2}$$

where $\lambda : [0,T] \to \mathbf{R}$ is continuous and the domain for z is the upper half plane denoted $\mathbf{H}=\{z \in \mathbf{C} : Im(z) > 0\}$. The Existence and Uniqueness Theorem from differential equations (see Appendix A1) tells us that every $z \in \mathbf{H}$ corresponds to some time interval $[0,t_0)$ such that a unique solution of (2) exists.

Now we develop an idea for the geometry of our domain. Suppose z_0 is a point such that the denominator of the right side of (2) is zero, i.e. $g(t,z_0) = \lambda(t)$. This results in the derivative, $\partial_t g(t,z)$, experiencing a singularity at that point; we can therefore conclude that z_0 is not in our domain. Under certain condition on λ (which we will look into later) we can guarantee that the

2

set of all such points produces a curve extending from the real axis. However, the curve may even be space filling, depending on the function λ. We will call this curve γ. To formalize this we set $T_z = \sup\{t_0 \in [0, T] : g(t, z) \; exists \; on \; [0, \; t_0)\}$. This gives us the largest possible value for t such that a solution, $g(t, z)$, makes sense. We now define $G_t = \{z \in \mathbf{H} : t < T_z\}$ which omits only the points in $\mathbf{H}$ that for some time $t < T_z$ cause $\partial_t g$ to become singular. G_t is now our domain for (2), see figure 1. It can be shown that G_t is actually a simply connected subdomain of $\mathbf{H}$ regardless of λ [10]. Below we will supply the conditions on λ such that the domain G_t is a quasislit-halfplane.[1] Since λ continuously generates a new map G_t for each subsequent value of t it follows that γ is also continuous in t. We can further define $\gamma(t)$ to be a curve in $\mathbf{H} \cup 0$ where $\gamma(0) = 0$ and $t \in [0, T]$. In general however, we can think of γ as a curve of singularities. It is interesting to note that since λ is real each point $z \in \gamma$ corresponds to a real valued g, thus γ is mapped to the real axis as can be seen in figure 1.
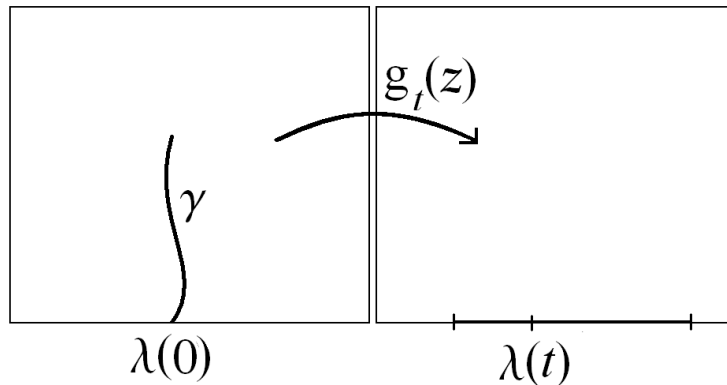

Figure 1: Forward Version. The slit γ is mapped to the real axis under g_t. The compliment of γ and the real axis in the left picture is G_t.

Since putting different driving terms into (2) (i.e. different functions in the place of λ) would result in a different function g we say that λ generates $g(t, z)$ and the corresponding domain G_z. Furthermore, λ is often called the driving term. You will also encounter the use of the notation $g_t(z)$ rather than $g(t, z)$, but they represent the same function. By the Riemann Mapping Theorem (see Appendix A1) it can be shown that g_t is a conformal map from G_z onto $\mathbf{H}$. This map can be made unique by specifying certain conditions on points in our domain. We usually think of this as having three degrees of freedom from which we can make the map unique. For our purposes we use choose these three degrees of freedom as follows: i) to map ∞ to ∞, ii) to map the real line to the real line and iii) to have the derivative evaluated at ∞ be 1. This is usually called the **hydrodynamic normalization** and more precisely states that:

---

[1]Technically this paper presents the conditions necessary in the backwards Loewner equation (see below); however the two results are equivalent [9].

3

$lim_{z\to\infty} g_t(z) - z = 0$, thus our map will look like the identity map when z is far away from the origin. Looking at the expansion of g_t we notice that all coefficients of z^n for $n \geq 2$ and the constant term must be zero, similarly the coefficient of z would have to be 1. So near infinity g_t has the form:

$$g_t(z) = z + \frac{c(t)}{z} + O\left(\frac{1}{z^2}\right)^2 \tag{3}$$

Often times the $c(t)$ term is referred to as the halfplane capacity and can be shown to be continually increasing in t (for more information see [8]). For those with a background in complex analysis, c is just the residue of g_t. Furthermore, since $g_0(z) = z$ it follows that $c(0) = 0$. We will find it useful to parameterize γ such that $c(t)$ is linear in t, so we choose $c(t) = 2t$. The reasoning behind this latter, seemingly arbitrary choice, is that in the radial version (which is the version that Loewner himself worked in) it is natural to parameterize γ such that $c(t) = e^t$. However, when we convert back over to the chordal version this e^t turns into $2t$. So it is more or less for historical purposes that we maintain the 2 in the parameterization. The halfplane capacity will play a large roll later when we model SLE.

Another term that you may come across is the *hull*. A hull in the upper half-plane is defined as a compact set $K \subset \overline{\mathbf{H}}$ so that $\mathbf{H}\backslash K$ is simply connected. As a technicality we need to further specify that $K = \overline{K \cap \mathbf{H}}$ which guarantees that K contains no intervals of $\mathbf{R}$ that are 'sticking out' to the left or right [8]. You can think of the hull as being, more or less, the generated curve γ. The term 'more or less' is used because the hull will not necessarily be a curve, it could be any set of points that satisfy the above definition like a space filling set. Notice that $G_t = \mathbf{H}\backslash K$. Sometimes you may see the K subscripted with a t. This is just there as a reminder that the hull is dependent on time.

2.2.2 Backward Loewner equation

We can think of the forward version of the Loewner equation as taking our curve γ and moving it down to the real axis as time moves forward. So we might infer that starting at our ending time T and progressing backwards to time 0 will result in the appearance of some curve γ from the previously 'empty' (at time T) upper-halfplane as in figure 2. Such functions are generated by the equation:

$$\frac{\partial}{\partial t} f_t(z) = \frac{-2}{f_t(z) - \xi(t)}, \qquad f_0(z) = z \tag{4}$$

where ξ is real and continuous. We call this the backward Loewner equation. One particularly nice part about equation (4) is that it has the whole upper half plane as a domain for every

---

[2]This last symbol is called a Landau symbol and denotes that the rate at which $O(\frac{1}{z^2})$ decreases is at least as fast as $\frac{1}{z^2}$.

generated function f_t. This contrasts from the relatively obscure domain observed in the forward version, which was the upper-half plane minus a curve γ (See figures 1 and 2).
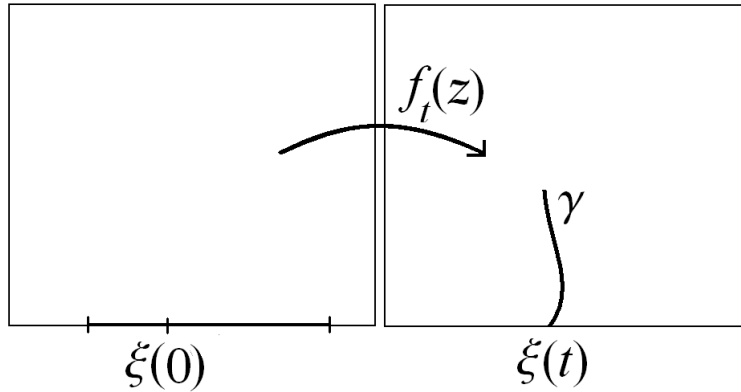

Figure 2: Backward Version. The bolded interval on the real axis is being mapped to γ under f_t.

Besides the obvious appearance of the negative sign in the numerator, equation (4) and equation (2) are related in another way in that if T is the largest possible value for t, then letting $\lambda(T - t) = \xi(t)$ brings us from one equation to the other. Although it seems entirely possible for the function f_t generated by (4) to be the inverse of g_t generated from (2), this is generally not true. Thus the curve γ generated by (4) is not necessarily the same curve γ generated by (2). However it is true that

$$f_T(z) = g_T^{-1}(z),$$

where T is the final time [10].

Subjecting our generated functions f_t to the same hydrodynamic normalization at infinity as we did above we get an expansion similar to that appearing in (3) except that the half-plane capacity term, $c(t)$, now has a sign opposite what had previously been observed. This can be thought of as a result of 'running time backwards' and replacing all t's with $-t$'s. Similarly, if γ is parameterized in the same way as in (2), then the expansion of f has the form:

$$f_t(z) = z + \frac{-c(t)}{z} + O\left(\frac{1}{z^2}\right) \tag{5}$$

As stated above for the forward version we observe that γ is mapped to the real axis. In the backward version we observe this same phenomenon in the opposite direction: part of the real axis is mapped to γ. In fact this mapping is two-to-one in nature, i.e. two points on from the real axis are mapped to one point on γ under f_t. This called welding and is easily observed by setting the driving term, ξ, equal to a constant. Letting $\xi(t) = A$ we can easily solve equation (4) by the method of separation of variables. Upon separating the variables in (4) we get:

$$(f - A)\partial f = -2\partial t.$$

Integrating and moving all terms to one side yields

$$\tfrac{1}{2}f^2 - Af + 2t + C = 0,$$

where C is a constant of integration. Now we turn to our companion the quadratic formula and solve for f

$$f = A \pm \sqrt{A^2 - 2(2t + C)}.$$

The initial value $f_0(z) = z$ tells us that $-2C = (z - A)^2 - A^2$, so we get

$$f_t(z) = A \pm \sqrt{(z - A)^2 - 4t}. \tag{6}$$

Now we look to see where the singular point $z = A$ is mapped to, we see that $f_t(A) = A + i2\sqrt{t}$. This result and the continuity of ξ make it clear that the '$\pm$' in (6) must be in fact a '$+$' to ensure that our image is in the upper half plane. It is interesting to note that as time moves forward this singular point moves upward along the line $Re\ (z) = A$; thus γ is perpendicular to the real axis. We can now easily observe the welding phenomenon. This describes how two real-valued curves, one on either side of $z = A$, are 'welded' together to form γ. To see this we set $f_t(z) = A$, then solving for z in (6) gives $z = A \pm 2\sqrt{t}$. Since t is positive these values are on the real axis and are centered symmetrically around A. Thus we see the two-to-one correspondence between the real axis and γ.

In general, the solutions for nonconstant driving terms are implicit and in the rare case that they are not the derivation of an explicit formula is rather involved. In light of this, we will refrain from direct calculation of formulas and merely state the result. We refer the reader to [6] for these derivations. If we set $\xi(t) = 2\sqrt{\kappa(1 - t)}$ we observe some very interesting features. The value of κ has a direct relation with the geometry of γ. When $\kappa < 4$ we get a simple curve that resembles a logarithmic spiral. However, when $\kappa = 4$ γ hits the real line. It is quite interesting to note that the measure of the angle at which this intersection occurs is 0! As κ grows to be greater than 4 we continue to observe contact with the real axis and the point of contact approaches $-\infty$ as $\kappa \to \infty$.

Now we will jump back to the forward version in (2). If we set $\lambda = \tfrac{3}{2} - \tfrac{3}{2}\sqrt{1 - 8t}$ then our line of singularities begins to trace out a semicircle centered at $\tfrac{1}{2}$ with a radius of $\tfrac{1}{2}$. It is easy
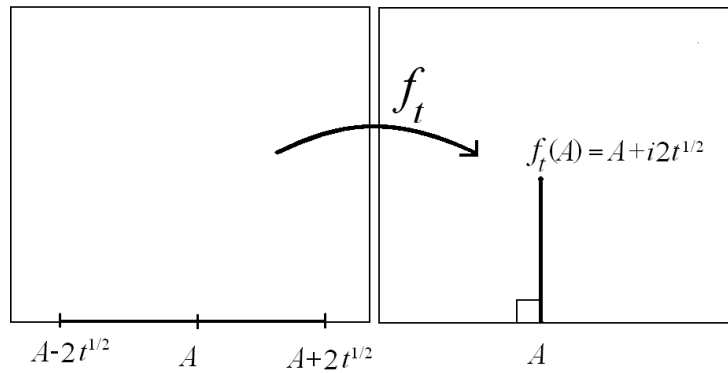
6

Figure 3: The welding property is easily observed in this example. We notice that f_t maps A to $A + i2\sqrt{t}$ and both of the points $A + 2\sqrt{t}$ and $A - 2\sqrt{t}$ to the point A resulting in a line segment perpendicular to the point A with a length of $2\sqrt{t}$.
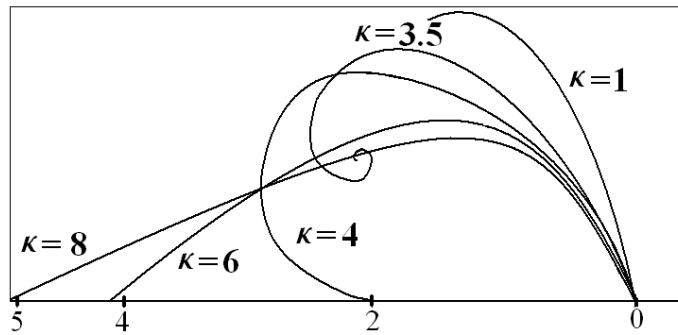

Figure 4: Here we see the behavior of the driving function $\xi(t) = 2\sqrt{\kappa(1-t)}$ for various values of κ.

to see that at time $t = \frac{1}{8}$ the generated curve contacts the real line. See [9] for a more thorough derivation.

One particularly interesting case is when the driving term causes a spiral to generate. The curve is simple until t reaches infinity and the curve hits back on itself and closes off the disk in the center. When a curve touches back on itself, the points completely enclosed by the curve all reach a singularity at the same time and thus the whole enclosed set is no longer part of the domain (see figure 5).

The last case to take note of is when the driving function is linear. In this case the generated curve emanates orthogonally from the real axis but as time moves forward it develops a slight curve. See figure 6.
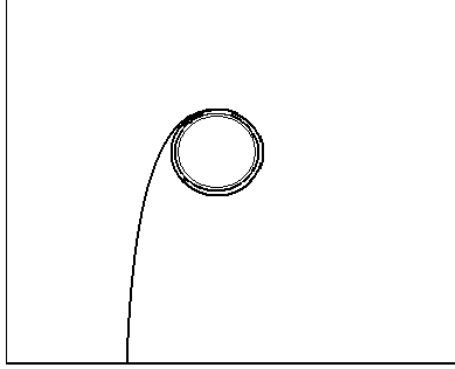
Figure 5: At t=∞ the disk inside of the spiral becomes closed off from the rest of the upper half plane. At this time every point within the disk results in a singularity.

3 Deriving the Loewner Equation

In this section we verify that upon correct parameterization g_t satisfies (2). We will state this more formally as a theorem below but for now we will investigate a few preliminary topics.

3.1 The scaling and summation rules

The scaling rule. For $r > 0$ consider the normalized, and thus unique, conformal map g_{rt}. The notation represents a hull at time t being scaled by a parameter r to yield a new hull at time rt. To visualize how this works take for example a hull, K_0, which is the vertical line segment extending from 0 to i, let t_0 denote the corresponding time. Now the hull rK_0 will represent the vertical segment from 0 to ri and is mapped by the function g_{rt_0} (see figure 7).

So in general the multiplication of r simply scales all points of K by r. The function $g_{rt}(z)$ then takes $\mathbf{H}\backslash rK$ to $\mathbf{H}$. However, the function $g_t(z/r)$ also takes $\mathbf{H}\backslash rK$ to $\mathbf{H}$. To understand this refer again to our example hull, K_0. The conformal map taking $\mathbf{H}\backslash rK_0$ to $\mathbf{H}\backslash K_0$ is z/r. So if we take the composition: $g_{t_0}(z) \circ (z/r) = g_{t_0}(z/r)$ we get a conformal map from $\mathbf{H}\backslash rK_0$ to $\mathbf{H}\backslash K_0$ and then to $\mathbf{H}$. This reasoning can be applied to any hull K.

Let us now look again at our composite function $g_t(z/r)$. Examining the series expansion we see that this function no longer satisfies the hydrodynamic normalization[3]:

$$g_t(z/r) = z/r + \frac{-c(t)}{(z/r)} + O\left(\frac{1}{(z/r)^2}\right) = z/r + \frac{-c(t)r}{z} + O\left(\frac{1}{(z)^2}\right).$$

---

[3]It is important to remember here that this does not mean our results are invalid, it just means that we need to make some corrections to $g_t(z/r)$ to ensure that it is unique and satisfies the Loewner equation.
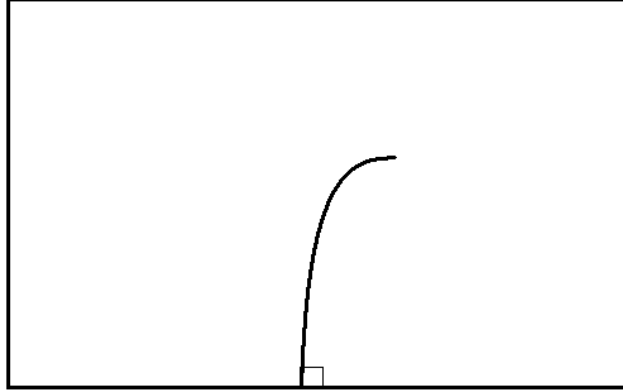
Figure 6: The above figure illustrates the curve generated by a linear driving function. Notice the bend toward the top.
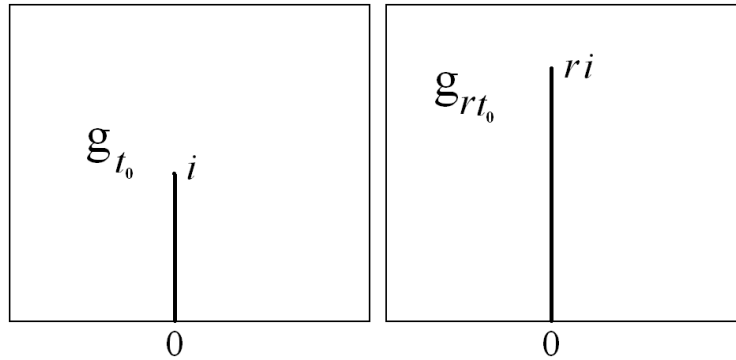

Figure 7: On the right is the hull K_0. The left is rK_0, the image of K_0 after scaling by a factor of r.

The presence of the r in the last two terms does not affect the behavior of $g_K(z/r)$ near ∞, the only place where it is a bother is its appearance as a coefficient of the linear term (recall that the hydrodynamic normalization requires our function have no constant term near ∞). The solution to this problem is simple: multiply by r. We now have two functions that map $\mathbf{H} \backslash rK_0$ to $\mathbf{H}$ and since they have each been made unique via normalization it follows that they are equal: $g_{rt}(z) = rg_t(z/r)$. Similarly we get that their respective capacities are unique, thus giving us the *scaling rule*:

$$c(rt) = r^2 c(t).$$

The summation rule. For the purposes of this derivation we will resort to a slightly different notation. Consider two hulls J and K such that $J \subset K$. Define their respective normalized conformal maps to be g_J and g_K. The subscripted notation can be thought of as
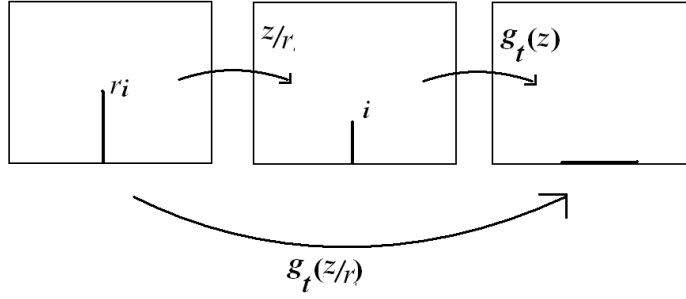
9

Figure 8: The figure above gives a schematic for the composition $g_{t_0}(z) \circ (z/r) = g_{t_0}(z/r)$ applied to rK_0.
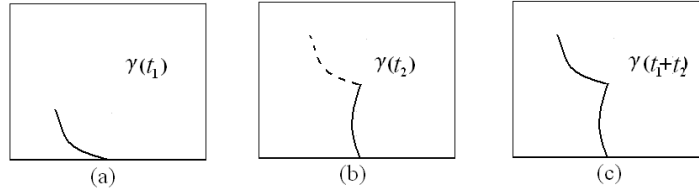

Figure 9: (a) represents the domain that g_L takes to $\mathbf{H}$. In (b) g_J takes the filled in curve to the real axis. In (c) g_K represents the composition of g_J and g_L and takes the filled in curve to the real axis.

representing the times, t_1 and $t_1 + t_2$, it takes to run g_t such that we get the respective hulls J and K. We then construct a new hull $L := \overline{g_J(K \backslash J)}$. L is then the image of the part of K that is not in J under g_J and can be thought of as corresponding to time t_2. Now if we compose g_J with g_L and apply it to the hull K, then g_J will map the 'J part of K' to the real axis and g_L will map everything that is left over to the real axis. We now have two functions that map $\mathbf{H} \backslash K$ to $\mathbf{H}$, namely $g_L \circ g_J$ and g_K. We already know that g_K has the correct normalization. To see that $g_L \circ g_J$ also satisfies the hydrodynamic normalization we note that since there are no constant terms in either g_L or g_J (they were both assumed to be hydrodynamically normalized at infinity) and since the only linear term appearing in their composition comes from composing the linear terms in each, we are done. So by uniqueness $g_L \circ g_J = g_K$. Looking at the capacities of these we recover the *summation rule*:

$$c(K) = c(J) + c(L).$$

So if we have two hulls $J \subset K$ we can create another hull L as defined above and the capacity of the larger hull, K, is the sum of the capacities of the two smaller hulls, J and L. In terms of t, this result can also be written as:

$$c(t_2 + t_1) = c(t_2) + c(t_1).$$

10

3.2 Derivation

Suppose that $\gamma(t) \in \overline{\mathbf{H}}$ is continuous such that $\gamma(0) \in \mathbf{R}$. Furthermore, impose the condition that if γ hits back on itself or on the real line then it immediately 'bounces back' into $\mathbf{H}\backslash K$ (for a more precise statement see [8]). It then follows that the associated capacity, $c(t)$, is continuous. Similarly, $\lambda(t) := g_t(\gamma(t))$ is also continuous. *Remark:* This definition of λ differs than the one presented in the Section 1 because the functions g_t may not have the correct normalization yet. For more information see [8]. The important attribute of the continuity of c is that we can now parameterize γ in virtually any continuous fashion. Now we can prove that g_t satisfies the Loewner equation and that λ is the driving term.

Theorem. Let $\gamma(t)$ be parameterized such that $c(t) = 2t$. Then for all $z \in \mathbf{H}\backslash K_t$, where K_t is the hull associated with $\gamma(t)$, then $g_t(z)$ satisfies

$$\tfrac{\partial}{\partial t} g_t(z) = \tfrac{2}{g_t(z) - \lambda(t)}, \qquad g_0(z) = z,$$

Proof: We will proceed in the manner suggested by Karl Fredrickson and begin with the Poisson integral formula in the upper-halfplane (see Appendix A3):

$$W(z) = \frac{1}{\pi} \int_{-\infty}^{\infty} \frac{1}{s^2 + 1} \frac{sz + 1}{s - z} Im\ W(s) ds + C. \tag{7}$$

Now consider the function $h_{\tau t} := g_\tau \circ g_t^{-1}$ for $\tau < t$. Notice that as a consequence of the summation rule when $t - \tau$ is small, $h_{\tau t}$ maps $\mathbf{H}$ to $\mathbf{H}\backslash\delta_{\tau t}$, where $\delta_{\tau t}$ is some small slit emanating from the real axis. The function $h_{\tau t}(z) - z$ satisfies the requirements for Poisson integral formula, so we now have:

$$h_{\tau t}(z) - z = \frac{1}{\pi} \int_{-\infty}^{\infty} \frac{1}{s^2 + 1} \frac{sz + 1}{s - z} Im\ (h_{\tau t}(s) - s)\ ds + C = \frac{1}{\pi} \int_{-\infty}^{\infty} \frac{1}{s^2 + 1} \frac{sz + 1}{s - z} Im\ (h_{\tau t}(s))\ ds + C. \tag{8}$$

The extra s on the right side of (8) evaluated to zero because $Im\ s = 0$ on the real line. Using the hydrodynamic normalization we can solve for C. Since $h_{\tau t}(z) - z$ should be zero at ∞ it follows that

$$0 = \frac{1}{\pi} \int_{-\infty}^{\infty} \frac{s}{s^2 + 1} Im\ h_{\tau t}(s) ds\ +\ C, \tag{9}$$

which gives

$$h_{\tau t}(z) - z = \frac{1}{\pi} \int_{-\infty}^{\infty} \left(\frac{1}{s^2 + 1} \frac{sz + 1}{s - z} - \frac{s}{s^2 + 1} \right) Im\ h_{\tau t}(s) ds. \tag{10}$$

Combining the fractions simplifies this expression to

$$h_{\tau t}(z) - z = \frac{1}{\pi} \int_{-\infty}^{\infty} \frac{Im \ h_{\tau t}(s)}{s - z} ds. \tag{11}$$

Everywhere except for on the slit $\delta_{\tau t}$, h maps to the real line and thus the imaginary part is zero. We can now change our bounds of integration from all of $\mathbf{R}$ to just over $\delta_{\tau t}$. Since $\lambda(t)$ is assumed to be continuous we can take $t - \tau$ to be as small as we want and thus we can make $\delta_{\tau t}$ into an arbitrarily small interval containing $\lambda(t)$.

In Appendix A3 the following expression is formulated:

$$c = \frac{1}{\pi} \int_{-\infty}^{\infty} Im \ W^{-1}(t) dt, \tag{12}$$

where c is the halfplane capacity of W. Since we have assumed the capacity of g_t to be $2t$, by the summation rule we get that the capacity of $h_{\tau t}^{-1}$ is the sum of the capacities of g_τ and g_t^{-1}, namely $2(\tau - t)$. Putting $h_{\tau t}$ into (12) gives:

$$\tau - t = \frac{1}{2\pi} \int_{-\infty}^{\infty} Im \ h_{\tau t}(s) ds. \tag{13}$$

By the same argument as above the bounds of integration on (13) can be reduced to the interval $\delta_{\tau t}$. Now divide equation (11) by equation (13):

$$\frac{h_{\tau t}(z) - z}{\tau - t} = \frac{2 \int_{\delta_{\tau t}} \frac{Im \ h_{\tau t}(s)}{z - s} ds}{\int_{\delta_{\tau t}} Im \ h_{\tau t}(s) ds}. \tag{14}$$

Since the integration is with respect to s we can substitute $g_t(z)$ in for z, giving

$$\frac{g_\tau(z) - g_t(z)}{\tau - t} = \frac{2 \int_{\delta_{\tau t}} \frac{Im \ h_{\tau t}(s)}{g_t(z) - s} ds}{\int_{\delta_{\tau t}} Im \ h_{\tau t}(s) ds}. \tag{15}$$

We can think of the denominator of (15) as normalizing the integral so that as we allow $\tau - t \to 0$ we are essentially integrating the function $2/(g_t(z) - s)$ against the Dirac delta function centered at $\lambda(t)$ (see Appendix A3). This just gives the value of $2/(g_t(z) - s)$ evaluated at $s = \lambda(t)$. Finally we come to

$$lim_{\tau \to t} \frac{g_\tau(z) - g_t(z)}{\tau - t} = \frac{\partial}{\partial t} g_t(z) = \frac{2}{g_t(z) - \lambda(t)}. \tag{16}$$

Q.E.D.

4 SLE

This section is designed to supply basic information pertaining to Brownian motion and SLE.

4.1 Probability and Brownian Motion

First we review some basic concepts of probability. If $f(x)$ is a given probability density function, then we define the **expectancy** of a continuous random variable X as $E[X] = \int_{-\infty}^{\infty} xf(x)$. We can further define the variance as $Var(X) = E[X^2] - (E[X])^2$. In less technical terms, the expectancy, E, is nothing more than the mean and the variance is the standard deviation squared. Furthermore, for any real-valued function g we get: $E[g(X)] = \int_{-\infty}^{\infty} g(x)f(x)$. It is beneficial to note that $E[aX + b] = aE[X] + b$ and $Var(aX + b) = a^2 Var(X)$, where a and b are constants (we leave the proof as an exercise for the reader). If an event occurs with a probability of 1 then they are said to occur **almost surely**, often abbreviated **a.s.**. This is analogous to saying that the probability of the event *not* happening has measure 0.

Brownian motion. Brownian motion is a phenomenon named after Scottish biologist Robert Brown, who in 1827 was observing particles in fluid and noticed very erratic behavior. This behavior appeared to be completely random and puzzled many people for some time. In 1905 Einstein showed that this motion of the particles was due to their interference with the molecules in the fluids. Later, in 1927 Norbert Wiener gave a mathematical description of Brownian motion.

To model Brownian motion we need to first understand its behavior. We begin by imagining a random walk. A one-dimensional random walk can be constructed in the following manner. Suppose that we begin at the origin at time 0. Now suppose that every time one minute has passed we flip a coin. If the coin lands on heads then we take a step forward, if the coin lands on tails we take a step backwards. Our motion is now a random walk. At any given point in time we have an equal probability of stepping forwards or backwards, thus our future path is not affected by where we came from. Upon scaling this random walk as illustrated below in figure 10^4 we can allow the time in between coin flips to approach 0. As this happens our motion approaches the process we call Brownian motion, denoted B_t (sometimes authors use W rather than B to pay tribute to Wiener, but they both represent the same process).

To reiterate, let $\{\mu_j\}$ be a sequence of independent, identically distributed random variables with mean 0 and variance 1. For $n > 0$ define the following sequence of functions

$$B_n(t) := \frac{1}{\sqrt{n}} \sum_{j=1}^{\lfloor nt \rfloor} \mu_j. \tag{17}$$

---

[4]This scaling is to ensure that random walk converges to Brownian motion as $\delta \to 0$.
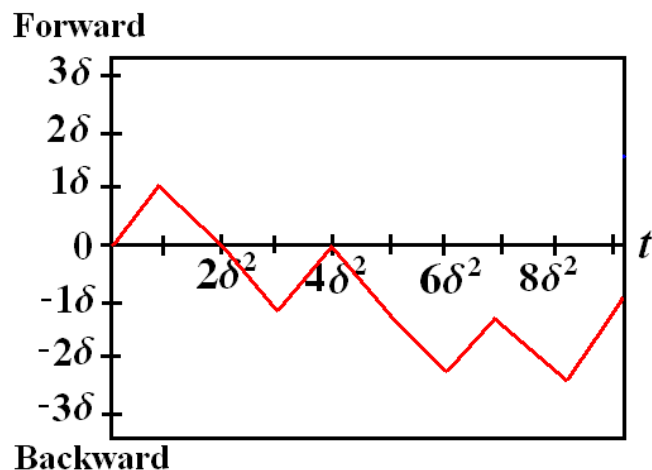
Figure 10: The red line represents a random walk. Notice how the time axis is scaled.

Thus $B_n(t)$ is a random variable that increases $\mu_j/\sqrt{n}$ for every increment in time where. Since the μ_j's are independent it follows that the time increments of $B_n(t)$ are also independent. In accordance with the above example we can choose the μ_j's to give either +1 or -1. This is a mathematical description of taking a step forward or backward at given time intervals and will be denoted by $\sum \pm 1$. With a little more work (which we do not include here), it can be shown that $B_n(t) \to B_t$ as $n \to \infty$. It also follows that Brownian motion is a continuous process. More surprisingly however, it can also be shown that it is nowhere differentiable! It has sharp cusps at every point on every scale! Now we state the three properties that characterize Brownian motion:

1. the manner in which we increment is independent of time,

2. the initial point is arbitrary ($B_t - B_s$, for $t \geq s$, is independent of s) and

3. it has a mean of 0 (if $B_0 = 0$) and a variance of t when the time change is t unit and when the motion is normally distributed.

Scaling Property of B_t. The scaling property of Brownian motion states that

$$B_t =^D aB_{t/a^2}. \tag{18}$$

The $=^D$ notation denotes an equivalence in distribution. This property follows from our initial scaling of B_t. If we substitute na^2 for n into equation (17) then we see that

$$B_{na^2}(t) = \frac{1}{a^2\sqrt{n}} \sum_{j=1}^{\lfloor na^2 t \rfloor} \mu_j. \tag{19}$$

14

Now define a new variable $s = a^2 t$ and substitute

$$B_{na^2}(s/a^2) = \frac{1}{a^2\sqrt{n}} \sum_{j=1}^{\lfloor ns \rfloor} \mu_j. \tag{20}$$

Since this last expression is just $\frac{1}{a}B_n(s)$ letting $n \to \infty$ gives us the scaling property.[5]

4.2 Brownian motion and SLE

SLE stands for Stochastic Loewner Equation (although you may also see it referred to as Schramm Loewner Evolution) and is created by allowing the driving in the Loewner equation to be Brownian motion. More explicitly we set the driving term to be $\xi(t) = \sqrt{\kappa}B_t$, where κ is taken to be positive and real valued. It turns out that different values of κ give us different families of generated curves. When κ is small the curves are simple (meaning they do not touch back on themselves or the real line). However when κ ranges between 4 and 8 we begin to see the curve coming into contact with itself and the real line. When $\kappa \geq 8$ then the generated curve is space filling! On a side note, there are two things that may prove to be beneficial to point out. The first is that $\mathrm{Var}[\sqrt{\kappa}B_t] = \kappa Var[B_t] = \kappa t$, which follows directly from the properties of variance. The second is that the Hausdorff dimension of SLE_κ for $\kappa < 8$ is $1+\frac{\kappa}{8}$.

O. Schramm and others have used SLE to aid in the study of a variety of physical phenomena including DLA (diffusion limited aggregation), the theory of random walks and percolation [7]. Listed below are some values for κ whose resulting SLE is the converging limit for the given random walk:

- LERW or Loop Erase Random Walk $\to$ SLE_2

- SAW or Self Avoiding Walk[6] $\to$ $SLE_{8/3}$

- Harmonic Explorer[7] $\to$ SLE_4

- Percolation $\to$ SLE_6

- Peano Curve or Uniform Spanning Tree $\to$ SLE_8

---

[5]To prove this in a more formal setting we would need to use some more machinery and look into what is actually meant to 'converge to Brownian motion.' However these calculations illustrate the basic idea behind the derivation.

[6]This is the only result listed that has not been proven, however it has been shown that if $SLE_{8/3}$ is the converging limit of a process then the process must be SAW. SAW is a process that is used to describe polymers [7].

[7]Presently this process has no physical interpretation however since SLE_4 is so essential this random walk was constructed.

15

SLE_κ allows us a way to model these random physical processes (e.g. LERW, SAW, etc.) which have been observed in many areas of the physical sciences, but have proven to be very difficult to understand.

5   Approximation

In the above section we discussed how the composition of different maps generated by the Loewner equation have some nice properties. In this section we examine how these properties can be exploited to generate virtually any function we want and then we will look into exactly how this can be used in approximating SLE.

5.1   Composition and the construction of maps

This section contains material which the reader may be unfamiliar with, in which case we refer them to Appendix A2. Furthermore, this section is structured toward the proof of the following theorem taken from [9]:

Theorem 1. If $\xi \in \text{Lip}\left(\frac{1}{2}\right)$ with $\|\xi\|_{\frac{1}{2}} < 4$, then $f_t(\mathbf{H})$ is a quasislit-halfplane for all t, where f_t are the maps generated by ξ.

Keeping this in the back of our minds let us continue on our path of *functional creation*!

5.1.1   General idea

What we want to do is approximate the generated function f by a series of functions f^n such that $f^n \to f$ as $n \to \infty$. We do this by first approximating the driving function ξ. Take for instance an arbitrary $\xi(t)$ (see the blue curve in figure 11). We must necessitate that ξ be continuous in t, however it does not have to be differentiable (recall that Brownian motion is nowhere differentiable). Now divide the time axis into equal n equal intervals located a distance of δ^2 apart and sample the ξ at each point. In other words, pick out the points on ξ corresponding to each time increment. We now connect these points with straight lines as illustrated by the red curve in figure 11. What we have done is approximated ξ by linear terms.[8] Let ξ_δ denote this new function made up of the straight line segments. Notice that as $\delta \to 0$ these linear approximations approach the function ξ.

---

[8]This approximation is linear because consecutive points are connected by lines and not curves. When we model SLE we will use square roots instead. However both ways work just the same as $\delta \to 0$, so we are free to use which ever method best fits the circumstances.
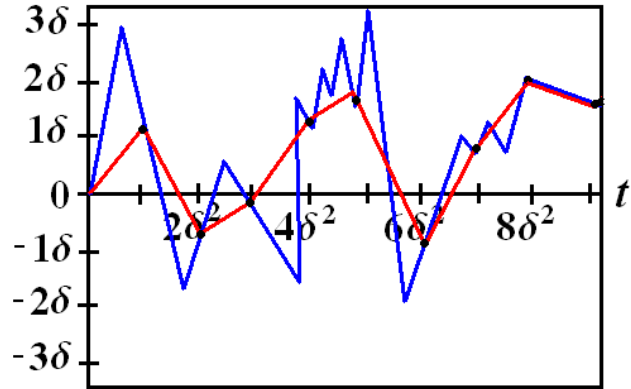
Figure 11: The blue line is $\xi(t)$ and the red line approximates it by connecting the points of ξ evaluated at $n\delta$.

Let f be the function generated by ξ and let the blue curve in figure 12 be the generated hull. Due to our continuity assumptions, if we use ξ_δ as a driving function we notice that the corresponding generated map, f_δ, approximates f; and furthermore, since $\xi_\delta \to \xi$ it is reasonable to believe that $f_\delta \to f$ as $\delta \to 0$ (we will prove this below). Notice how the image of the straight approximating lines of figure 11 now appear as curved lines in figure 12. This is because a linear driving function generates a curve with a slight bend to it (see figure 6).
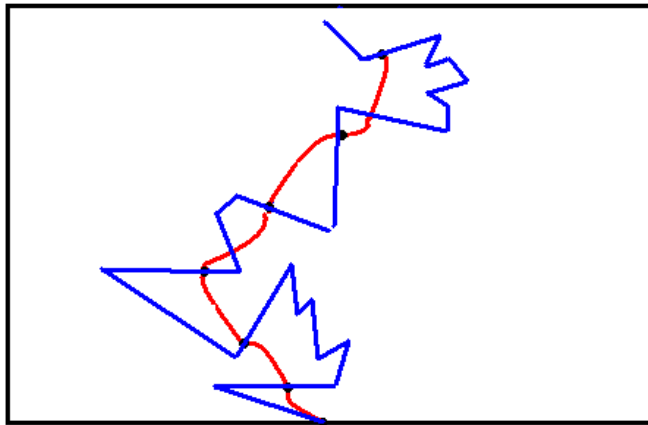

Figure 12: The blue line is the curve generated by ξ and the red line is the curve generated by the approximating function. Notice how the straight lines from figure 11 generate curved lines here.

Yet the question remains: How can we construct f_δ? This is where the summation rule comes in. Number each curve of ξ_δ from 1 to n as illustrated in 13. Recall that since this is the backward

17

version what we see in figure 13 is at the final time T. Now just look at the curve labeled n. Imagine rewinding time so that curves 1 through $n-1$ are on the real axis, but curve n is still in the upper-halfplane, call this domain D_n. The Riemann Mapping Theorem (see Appendix A1) tells us that there exists some conformal map from the upper-halfplane to D_n, call it ϕ_n.
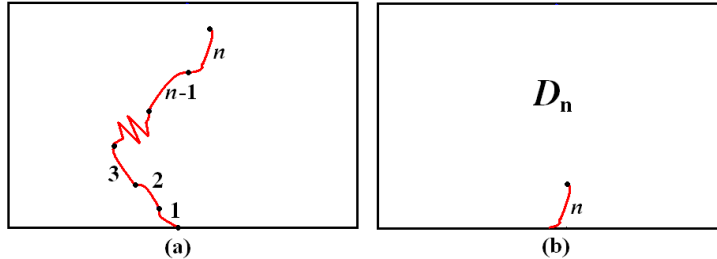

(a) (b)

Figure 13: (a) illustrates the generated curve from the approximating function. Each segment corresponding to the numerical time increments at which ξ was sampled is numbered from 1 to n. Figure (b) is attained by running time backwards and returning curves 1 through $n-1$ to the real line. Only the nth curve is left.

Now move time forwards a step of δ^2. We see both curves n and $n-1$ in $\mathbf{H}$, but the rest are still on the real line, call this domain D_{n-1}. Again, we know that there exists a conformal map from D_n to D_{n-1}, call it ϕ_{n-1}. Proceed in this manner until we have n maps: $\phi_n, \phi_{n-1}, \ldots, \phi_1$ that each increment f_δ a time step of δ^2. Now by taking the composition of these maps the summation rule tells us that the resulting function is exactly the function that we are looking for. In other words: $f_\delta = \phi_n \circ \phi_{n-1} \circ \ldots \circ \phi_1$. So as $\delta \to 0$ the $\phi_n \circ \phi_{n-1} \circ \ldots \circ \phi_1 \to f$!

5.1.2   Beneficial lemmas

We will use the same concepts of the previous section to prove Theorem 1. The notation is slightly different at times, however it is the exact same idea as the general argument given above. Again, this proof requires some background on a variety of concepts (Hölder continuity, quasiconformal maps, etc.) which are all discussed in Appendix A2. We will begin by the statement of some lemmas.

Suppose that the image of f_t is a quasislit-halfplane, then $\gamma(t)$ only intersects the real axis once. This occurs when $t = 0$ so we can extend $f_t(z)$ to be continuous for all $z \in \mathbf{H} \cup \mathbf{R}\backslash\xi(0)$. Thus $x(t) := (f_t(x)$ satisfies:

$$\frac{\partial}{\partial t}x(t) = \frac{-2}{x(t) - \xi(t)}, \qquad x(0) = x_0 \tag{21}$$

where $x_0 \in \mathbf{R}\backslash\xi(0)$.

In reference to this "real version" of the Loewner equation, J. Lind proceeds to prove the following lemmas in [9].

18

Lemma 1. Let $\xi \in \text{Lip}\left(\frac{1}{2}\right)$ with $\|\xi\|_{\frac{1}{2}} < 4$ and $\xi(0) = 0$. Suppose that $x(t)$ is a solution to (5), with $x_0 \neq 0$. Then $C_1 x_0^2 \leq T(x_0) \leq C_2 x_0^2$, where C_1 and C_2 are positive, finite and depend on the value of $\|\xi\|_{\frac{1}{2}}$.

This says that for $\|\xi\|_{\frac{1}{2}} < 4$ there exists some time $T(x_0) < \infty$ such that $x(T) = \xi(T)$, where x is a solution to (5), and thus resulting in a singularity at that point.

In Lemma 3 of [9], J. Lind shows that for each time $T < \infty$ there are exactly two initial points x_0 and y_0, where $x_0 < \xi(0) < y_0$ such that their corresponding solutions to (1), x and y, both equal $\xi(T)$ at the same time T.

From this we can define the welding homeomorphism $\psi : \mathbf{R} \to \mathbf{R}$ to be the orientation-reversing map that satisfies $\psi(x) = y$ if and only if $x(T) = y(T)$ and thus interchanges the two points that hit the singularity ξ at the same time. The following lemma supplies us with some estimates on ψ.

Lemma 2. Let $\xi \in \text{Lip}\left(\frac{1}{2}\right)$ with $\|\xi\|_{\frac{1}{2}} < 4$ and $\xi(0) = 0$. There exists some constant $A_0 > 0$, depending only on $\|\xi\|_{\frac{1}{2}}$, so that if $0 \leq x < y < z$ with $y - x = z - y$, then

$$\frac{1}{A_0} \leq \frac{\psi(x) - \psi(y)}{\psi(y) - \psi(z)} \leq A_0 \tag{22}$$

We will use the following lemma to tie in Lemmas 1 and 2 in the crux of the proof to Theorem 1.

Lemma 3. $\mathbf{H} \backslash \gamma[0, T]$ is a quasislit-halfplane if and only if there is a constant $1 \leq M < \infty$ such that

$$\frac{1}{M} \leq \frac{x - \xi(0)}{\xi(0) - \psi(x)} \leq M \tag{23}$$

for all $x > \xi(0)$ and

$$\frac{1}{M} \leq \frac{\psi(x) - \psi(y)}{\psi(y) - \psi(z)} \leq M \tag{24}$$

whenever $\xi(0) \leq x < y < z$ with $y - x = x - y$. Furthermore, the quasislit constant K of $\mathbf{H} \backslash \gamma[0, T]$ depends on M only.

In the next section we repeat the argument outlined in Section 5.1.1 but in a more rigorous manner.

19

5.1.3 Proof of Theorem 1

Proof: First we will construct an approximation of the driving term and then show that the image of this approximation is a slit-halfplane. Then we will show that this approximation satisfies the hypothesis of Lemma 3 and thus the image is a K-quasislit-halfplane. But since the space of K-quasislit-halfplanes is compact we know that the limiting function is also a K-quasislit-halfplane and is therefore a slit-halfplane, thus completing the proof.

Due to the scaling invariance of ξ we have a large amount of freedom when it comes to parameterizing γ, so if we can show that the image at time 1, $f_1(\mathbf{H})$, is a quasislit-halfplane, then we will be done.[9] We can approximate the Loewner equation by first taking the composition of n infinitesimal conformal maps, ϕ^k, and then making an estimate [12]. In order to do this we must first approximate our driving term ξ, which is assumed to be $\mathrm{Lip}\left(\frac{1}{2}\right)$, by some functions $\xi^n \in \mathrm{Lip}\left(\frac{1}{2}\right)$ which we already know generate quasislit-halfplanes. More precisely, we want to construct $\xi^n \in \mathrm{Lip}\left(\frac{1}{2}\right)$ so that $\xi^n(t_k) \to \xi(t_k)$ as $n \to \infty$, where $n \in \mathbf{N}$, $t_k = k/n$ and $\|\xi^n\|_{1/2} \le \|\xi\|_{1/2}$. This last inequality is necessary to ensure that our approximation of ξ has a $\mathrm{Lip}\left(\frac{1}{2}\right)$ value that is less than or equal to the $\mathrm{Lip}\left(\frac{1}{2}\right)$ value of ξ. Otherwise we may exceed our upper $\mathrm{Lip}\left(\frac{1}{2}\right)$ bound of 4. Furthermore, the n appearing in the above relations is a factor that will be allowed to approach ∞ in order to yield our desired infinitesimal estimates.

We are going to construct linear driving functions (in contrast to the square root ones used below for the program). To do this we set $m_k = n(\xi(t_{k+1}) - \xi(t_k))$ and to incorporate a continuous time parameter $t \in [0,1]$ let $\xi^n(t) = m_k(t - t_k) + \xi(t_k) = \xi(t_{k+1})(t - t_k) + \xi(t_k)(1 + n(t_k - t))$. A key concept that we gather from this formulation is that as $t \to t_k$, $\xi^n(t) \to \xi(t)$; in other words, our approximating functions approach our desired function. To verify that $\|\xi^n\|_{1/2} < 4$ we choose $(x,y) \in [t_k, t_k + 1]$ for some nonnegative k. We now notice that $|\xi^n(y) - \xi^n(x)|$ reduces to $\left|(y - x)(\xi\left(\frac{k+1}{n}\right) - \xi\left(\frac{k}{n}\right))\right|$, but when $|y - x| \le 1$ we have that $|y - x| \le \sqrt{|y - x|}$ and thus $|\xi^n(y) - \xi^n(x)| = \left|(y - x)(\xi\left(\frac{k+1}{n}\right) - \xi\left(\frac{k}{n}\right))\right| \le C\sqrt{|y - x|}$ for $|y - x| \le 1$ and some constant C. It then follows that ξ^n is Hölder continuous on $[t_k, t_k + 1]$. Now, without loss of generality, assume that $\xi^n(y) \ge \xi^n(x)$, then upon maximizing the function $h(x,y) := \xi_n(y) - \xi_n(x) - D\sqrt{|y - x|}$, where we set $D = \|\xi\|_{1/2}$ and $(x,y) \in [t_j, t_{j+1}] \times [t_k, t_{k+1}]$, we find that $h \le 0$ and thus $\|\xi^n\|_{1/2} \le \|\xi\|_{1/2}$ as desired since $\|\xi^n\|_{1/2}$ is the smallest value that C can take on.

Now we create our maps ϕ^k. Let ϕ_t^k denote the maps generated by $\xi^n(t_k + t) = m_k(t) + \xi(t_k) = n(\xi(t_{n+1}) - \xi(t_n))t + \xi(t_n)$ where $t \in [0, 1/n]$ and thus we have a linear driving term. This form of driving term results in a curve emanating perpendicularly from the real axis and then beginning to develop a curve as in figure 6. To ease up the notation a little, let $\phi^k := \phi_{1/n}^k$. Now if f_t^n is the map generated by ξ_n for $t \in [0,1]$, we have that f_1^n is the composition of n of our estimating

---

[9]For more information on scaling invariance see Proposition 2.1 in [13] and the comment before Lemma 1 in [9].

maps ϕ^{k_i} where $k_i \neq k_j$; in other words $f_1^n = \phi^n \circ \phi^{n-1} \circ \ldots \circ \phi^2 \circ \phi^1$. Since each ϕ^j yields a slit-halfplane, we can conclude that $f_1^n(\mathbf{H})$ is a slit-halfplane. Now we see that the hypothesis for Lemmas 1 and 2 are satisfied. Lemma 2 yields exactly the second condition in Lemma 3 whereas, with a little algebra, Lemma 1 offers exactly the first condition in Lemma 3. Therefore, by Lemma 3 $f_1^n(\mathbf{H})$ is a K-quasislit-halfplane and the eccentricity parameter K is independent of the value of n. Now if we impose the limit as $n \to \infty$ we get a sequence of functions, each of which results in a K-quasislit-halfplane. Since the space of K-quasislit-halfplanes is compact, we are guaranteed that this sequence has some subsequence which converges to a limit f_1 that also results in a K-quasislit-halfplane (which is slit-halfplane). This is our desired function. Q.E.D.

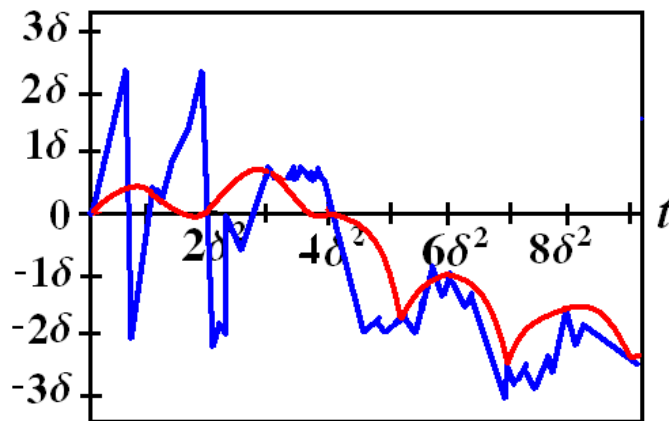## 5.2   Composition and approximating SLE

Figure 14: The blue curve is a sample of Brownian motion and the red curve is an approximation consisting of square root functions.

   Now we will use the ideas from the previous section to construct a usable model for generating SLE. Just as before we will begin by approximating the driving term, which in this case is $\sqrt{\kappa} B_t$, where B_t is Brownian motion. Since Brownian motion is a random process each time we run Brownian motion it looks different. Suppose that we have a sample of Brownian motion (see figure 14). Again, divide the time into equal increments and note the corresponding points on the curve. We are now going to connect these points, however this time we are going to use a square root function to connect them, rather than the linear connection used above and in 11. The reason for this will become clear in a moment. Again, we can put both the sample of Brownian motion and the approximating function into the Loewner equation to develop two similar curves in $\mathbf{H}$ (see figure 15). Now rewind time back to where the last approximating curve is the only

one present in the upper-halfplane. We now have a map generated by a square root driving term. We saw above that such a driving function results in a straight line emanating from the real axis at a certain angle $a\pi$. Now we want to find a conformal map from the upper-halfplane to this new domain. Well it just so happens that such a conformal map has a fairly easy representation and can be looked up in most tables. The map is:

$$f(z) = (z - a)^a(z - (a - 1))^{1-a} \tag{25}$$

where $a \in [0, 1/2]$ is the angle the line segment makes with the positive real axis divided by π. This simple representation is precisely why we chose to approximate Brownian motion with the square root function. Now all we need to do is gather the other $n - 1$ of these maps. So let time run forward a little until the second to last approximating function is completely exposed. Now we just use equation (25) again to get the conformal map that takes this slit to the real line. Continue this same process $n - 2$ more times and then as we saw above the composition of these maps results in an approximation of the generated curve. Letting $n \to \infty$ will finish the job.
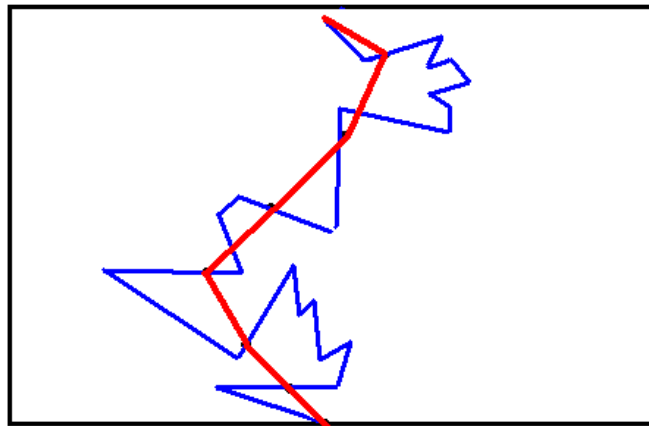

Figure 15: The blue line represents an SLE (a curve generated by Brownian motion) and the red line is approximating it. Notice how the approximations are straight lines. This enables us to use a known conformal map to construct the red curve.

6   The Program

This section discusses how the mathematics of the previous section is implemented to model SLE_κ on a computer. We will examine the original program by S. Rohde. Equation (25) gives us our desired conformal maps. The Taylor series of f at infinity looks like:
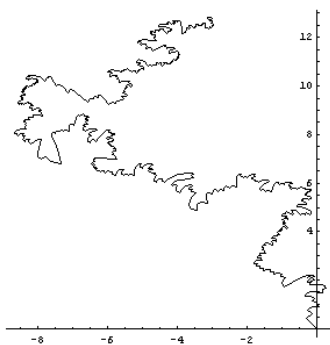
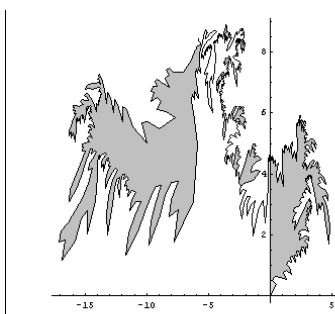Figure 16: Pictured above is a map generated by Mathematica for SLE_3.

Figure 17: For $\kappa > 8$ we get a space filling curve. In this approximation of SLE_8 we can begin to see this space filling behavior. The shaded in regions denote areas that have been 'closed off' and have simultaneously hit a singularity. Notice the periods where long, straight lines have emerged. In actuality these lines would have the sharper, more chaotic look that most of the other segments exhibit. The appearance of these lines increases with the value of κ and illustrates a flaw in the validity of the program.

$$f(z) = z + (1 - 2a) + \frac{\frac{1}{2}(a-1)a}{z} + \cdots \tag{26}$$

Now we want to look at the composition of n maps. For simplicity we fix a and define two maps: $f_1 := (z-a)^a(z-(a-1))^{1-a}$ and $f_2 := (z-(1-a))^{1-a}(z-((1-a)-1))^{1-(1-a)}$. f_1 is exactly equation (25) and thus creates a map with an angle between 0 and $\pi/2$ from the *positive* real axis. f_2 replaces every a with $1-a$ in (25) and thus creates the same angle between 0 and $\pi/2$ but this time with the *negative* real axis. The two functions create slits that are symmetric about the imaginary axis. Here is the expansion of f_2 to contrast the that of f_1 as given in (26):

$$f_2(z) = z - (1 - 2a) + \frac{\frac{1}{2}(a-1)a}{z} + \cdots \tag{27}$$

As you can see the only places in the first three terms where equations (26) and (27) differ is that the constant terms exhibit opposite signs. Now we make the approximating function, f_n,

23

out of n random compositions of these f_1 and f_2. In particular we take $F_n = g_1 \circ g_2 \circ \cdots \circ g_n$, where the g_i's are either f_1 or f_2 chosen with equal probability. It turns out that this function converges to SLE_κ. We can find the relation between κ and a in the following way. Let

$$g_1(z) = z + c_0 + \frac{c_1}{z} + \ldots$$
$$g_2(z) = z + d_0 + \frac{d_1}{z} + \ldots$$

be the expansions of two random g_i's, so g_1 and g_2 could each be either f_1 or f_2. When we compose these two maps the constant terms and the coefficients of the $1/z$ terms add:

$$g_1 \circ g_2(z) = z + (c_0 + d_0) + \frac{c_1 + d_1}{z} + \ldots \tag{28}$$

If we continue to compose more g_i's the residues (i.e. the coefficients of the $1/z$ term) will keep adding and since the residues of f_1 and f_2 are the same it follows that the residue of F_n is simply $n\frac{1}{2}(a-1)a$. Since we want to parameterize our function F_n so that the halfplane capacity (or residue) is $-2t$ it follows that $t = -n\frac{1}{4}(a-1)a$.

Looking at the constant term of F_n we see that, although the constant terms of the g_i have added, they are not all the same in that they differ by minus signs. This is actually a blessing in disguise. When we add n ± 1's together then we get a random walk with variance n. In fact this random walk is exactly $\sum \pm 1$ discussed above. So the constant term of F_n is now $(1 - 2a) \sum \pm 1$. If we take the variance of F_n then every term is considered a constant except for the constant term (kind of ironic) which is the only probabilistic element in F_n. Since $Var(a(\sum \pm 1) + b) = a^2 Var(\sum \pm 1)$ where a and b are constants, it follows that $Var(F_n) = n(1-2a)^2$ (see Section 4.1). Furthermore, we want F_n to approximate $\sqrt{\kappa} B_t$, so they both need to have the same variance. The variance of $\sqrt{\kappa} B_t$ is κt, so we get the expression: $n(1 - 2a)^2 = \kappa t = -\kappa n \frac{1}{4}(a-1)a$. Finally we have our equation for a

$$a = \frac{1}{2} \pm \frac{\sqrt{\kappa}\sqrt{16 + \kappa}}{32 + 2\kappa}. \tag{29}$$

Both of these solutions are symmetric around $1/2$ so just pick one: $a = \frac{1}{2} - \frac{\sqrt{\kappa}\sqrt{16+\kappa}}{32+2\kappa} = \frac{1}{2}\left(1 - \sqrt{\frac{\kappa}{16+\kappa}}\right)$.

Using this and the code below, we are able to generate curves that approximate SLE_κ.

```
\[Kappa] = 3.; a = 1/2 (1 - Sqrt[\[Kappa]/(16 + \[Kappa])]);
f1[x_] = (x - a)^a (x - (a - 1))^(1 - a);
f2[x_]  = (x - (1 - a))^(1 - a) (x + a)^a;


Nr = 1000;
```

```
data = {0.};
Do[
        If [Random[Integer] == 0, data = Flatten[Append[{0.}, f1[data]]],

      data = Flatten[Append[{0.}, f2[data]]]
       ],
    {Nr}
    ];


h[z_] = {Re[z], Im[z]};
Map[h, data];
ListPlot[%, PlotJoined -> True, AspectRatio -> 1]
```

\[Kappa] designates the value or κ and the `Nr` variable tells the program how many slit maps to compose. The composition is done in the `Do` loop and the variable `data` stores the points where consecutive slits connect. `ListPlot` is what actually plots the points in Mathematica.

7   Appendix A1

The Existence and Uniqueness Theorem tells us that under certain hypothesis on a particular initial value problem there exists a unique solution to that equation. Below we state it for a first order differential equation (notice that the Loewner equation is first order in time).

Existence and Uniqueness Theorem. Let ψ and $\partial\psi/\partial g$ be continuous in some rectangle $R = \{(t, g) : |t - t_0| < \alpha, |g - g_0| < \beta\}$, then there is some interval $|t| \leq a \leq \alpha$ in which there exists a unique solution $g = \phi(t)$ of the initial value problem:

$$\frac{dg}{dt} = \psi(t, y), \qquad g(t_0) = g_0. \tag{30}$$

This is also valid if g is a function of two variables as we encounter in the Loewner equation the only difference is that we would change the d into a ∂. For more information see [3].

The Riemann Mapping Theorem is a very powerful tool of complex analysis. It states that there to exists a conformal (one-to-one and analytic) map from virtually any simply-connected region to the unit disk.

Riemann Mapping Theorem. Suppose D is a simply-connected domain with at least two points in its boundary; let p be a point of D. Then there is a conformal function ϕ that maps D

onto the open unit disk and $\phi(p) = 0$. Furthermore, ϕ is uniquely determined by the requirement that $\phi'(p)$ be positive.

Some texts give other variations on this last uniqueness guarantee, but in general we have three degrees of freedom (i.e. three parameters which we can vary) on the function ϕ in order to guarantee its uniqueness. For the purposes of the Loewner equation we have used the hydrodynamic normalization, which says that at ∞ the function looks like z. So you can think of the point at ∞ as being the point p and the derivative there is 1 (which is positive) since the derivative of z is 1. Since we are guaranteed that we can map just about any domain to the unit disk by a one-to-one function it follows that we can map any simply-connected domain D to any other simply-connected domain C by a one-to-one analytic map. This is because every one-to-one function has an inverse. Let ϕ_D (resp. ϕ_C) be the function mapping D (resp. C) to the unit disk. By taking the composition $\phi_D \circ \phi_C^{-1}$ we get a one-to-one function from D to C. Furthermore, since the composition of two analytic functions is itself analytic it follows that $\phi_D \circ \phi_C^{-1}$ is conformal.

8 Appendix A2

This Appendix is primarily used as a supplement to arguments presented in Section 5.

8.1 Compact Spaces

Our first steps deal with expanding our notion of compact sets in $\mathbf{R}^n$ to the more general notion of compact spaces. Suppose S is a set such that given two points $\mathbf{x}$ and $\mathbf{y}$ in S there is an associated distance function $d(\mathbf{x}, \mathbf{y})$ which yields a nonnegative real number and satisfies:

1. $d(\mathbf{x}, \mathbf{y}) = 0 \iff \mathbf{x} = \mathbf{y}$,

2. $d(\mathbf{x}, \mathbf{y}) = d(\mathbf{y}, \mathbf{x})$ and

3. the triangle inequlality, $d(\mathbf{x}, \mathbf{y}) + d(\mathbf{y}, \mathbf{z}) \geq d(\mathbf{x}, \mathbf{z})$,

then S is a metric space [15]. For instance $\mathbf{R}^n$ and $\mathbf{C}$ are two examples of metric spaces. Now we can define S to be a compact space if every open cover of S has a finite subcover [5]. It follows then (for metric spaces) that every sequence in S has a convergent subsequence in S [1], this is often called sequential compactness and will play a role later.

8.2   Homeomorphisms

Two geometric figures or topological spaces are said to be homeomorphically equivalent if one can be distorted and deformed into the other in a continuous and one-to-one fashion. This distortion must also be invertible. For example, a square is topologically equivalent to a circle. However neither of these are topologically equivalent to an annulus because the annulus has a hole in it and there is no way to create a hole in a square or a circle without tearing it or gluing it. We call this type of mapping a homeomorphism.

8.3   Quasislit-halfplanes

To make precise the domains we will be considering we define the following:

Definition 1. A domain D is a *slit-halfplane* if it has the form $D = \mathbf{H}\backslash\gamma[0, t]$, where $\gamma(t) \in \mathbf{H} \cup \gamma(0)$ is some simple continuous curve with $\gamma(0) \in \mathbf{R}$.

We now ask the question: How do we know when the image of a function is a slit-halfplane? To answer this we start by using techniques from complex analysis. Conformal maps are very useful in the study of the Loewner equation, however, there exists a generalization of conformal maps that we will also find useful. These are called *quasiconformal maps*. To get an idea of what a quasiconformal map is, imagine a differentiable function mapping planer regions to planer regions that carry tiny circles to tiny ellipses. In the study of ellipses one often comes across the eccentricity value $e = \sqrt{1 - \frac{b^2}{a^2}}$ of an ellipse, where a and b denote the lengths of the semimajor and semimajor axis, respectively. This offers a way to determine how "eccentric" the ellipse is.

With quasiconformal maps we associate a similar notion of eccentricity, which we will denote by K and require that K be bounded. It must be understood that $K \neq e$; indeed even in the case of when a quasiconformal map takes circles to circles the corresponding eccentricity value K is 1. However, when an ellipse is actually a circle (i.e. $a = b$) the corresponding elliptic eccentricity e is 0.

Remark: When a quasiconformal map takes circles to circles, then the map is simply the usual conformal maps we have come to know and love; so in this way a quasiconformal map is a generalization of a conformal map. The boundedness of K implies that although angle measures are distorted under a quasiconformal mapping, this distortion is not arbitrary and is bounded throughout the domain [2]. To make this definition more precise we define the following:

Definition 2. Let f be a homeomorphism from $\mathbf{C}$ to $\mathbf{C}$. The *dilation* of f at a point z is given by

$$D_f(z) := \frac{|f_z| + |f_{\bar{z}}|}{|f_z| - |f_{\bar{z}}|} \geq 1, \tag{31}$$

and the *maximal dilation* of f is

$$K_f := \sup_z D_f(z). \tag{32}$$

The value for D_f is essentially representing the length of the semimajor axis divided by the length of the semiminor axis of the image of a circle under f–this image being an ellipse.

Definition 3. A homeomorphism $f : \mathbf{C} \to \mathbf{C}$ is said to be *quasiconformal* if K_f, as defined above, is finite. f is called $K - quasiconformal$ if the maximal dilation is equal to the eccentricity value; thus $K_f = K$.

From this we easily construct the following:

Definition 4. A *quasislit-halfplane* is the image of $\mathbf{H}\backslash[0, i]$ under a quasiconformal mapping fixing $\mathbf{H}$ and ∞.

Observe that since $\mathbf{H}\backslash[0, i]$ is simply-connected every quasislit-halfplane is also simply-connected. By a definition analogous to the one above we can construct a K-quasislit-halfplane as the image under a K-quasiconformal-homeomorphism. There are a few other criteria for this and the technicalities are presented in [12]. However, from their definition we can gather that not only is the space of quasislit-halfplanes a subset of slit-halfplanes, but more importantly that the space of K-quasislit-halfplanes (which is a subspace of quasislit-halfplanes) is compact [9].

8.4 Hölder Continuity

The concept of Hölder continuity will also play a role so we include the criteria: A function $\xi(t)$ defined on U is Hölder continuous if $|\xi(t) - \xi(s)| \leq C |t - s|^a$ for all $s, t \in U$ and where a and C are positive constants. $\text{Lip}\left(\frac{1}{2}\right)$ is the name we attribute to the space of Hölder continuous functions such that $a = \frac{1}{2}$, and we let $\|\xi\|_{\frac{1}{2}}$ denote the smallest value of C satisfying the above definition [9]. For the proof that the driving term is Hölder continuous in a quasislit-halfplane see [12].

Remark: Hölder continuity implies uniform continuity.

9 Appendix A3

Poisson's integral formula on the unit disk is given by:

$$U(w) = \frac{1}{2\pi} \int_0^{2\pi} \frac{e^{i\theta} + w}{e^{i\theta} - w} Re\ U(e^{i\theta}) d\theta\ +\ C, \tag{33}$$

where $C \in \mathbf{R}$ is a constant and U is analytic on $\mathbf{D} = \{w : |w| < 1\}$ and is extended to be piecewise continuous on $|w| = 1$. We now want to carry this equation over to the upper-halfplane. To do this we make use of the conformal map $w = \frac{z-i}{z+i}$ which takes the upper-halfplane to the unit disk with the real line going to $|w| = 1$. Since we are now going to be working in the halfplane instead of the disk we make the following definition: $W(z) := U\left(\frac{z-i}{z+i}\right)$ and thus W is analytic on $\mathbf{H}$ and continuous on $\overline{\mathbf{H}} \cup \infty$. Now rewriting (33) gives:

$$W(z) = \frac{1}{2\pi} \int_{-\infty}^{\infty} \left(\frac{\frac{t-i}{t+i} + \frac{z-i}{z+i}}{\frac{t-i}{t+i} + \frac{z-i}{z+i}}\right) \frac{2}{(t+i)^2} \frac{t+i}{t-i} Re\ W(t)\ dt\ +\ C, \tag{34}$$

where we have made the substitution: $e^{i\theta} = \frac{t-i}{t+i}$, whose derivative yields $e^{i\theta} d\theta = \frac{2}{(t+i)^2} dt$ and thus $d\theta = \frac{2}{(t+i)^2} \frac{t+i}{t-i} dt$. With some algebra equation (34) becomes the Poisson integral formula in the upper-halfplane:

$$W(z) = \frac{1}{2\pi} \int_{-\infty}^{\infty} \frac{2}{t^2+1} \frac{tz+1}{i(t-z)} Re\ W(t) dt\ +\ C = \frac{1}{\pi} \int_{-\infty}^{\infty} \frac{1}{t^2+1} \frac{tz+1}{t-z} Im\ W(t) dt\ +\ C. \tag{35}$$

We also take this time to point out another version Poisson's half-plane integral formula which is given by:

$$z - W^{-1}(z) = \frac{1}{\pi} \int_{-\infty}^{\infty} \frac{Im\ W^{-1}(t)}{z-t} dt, \tag{36}$$

where W is as defined above. Substitute $W(z)$ for z to get:

$$W(z) - z = \frac{1}{\pi} \int_{-\infty}^{\infty} \frac{Im\ W^{-1}(t)}{W(z) - t} dt. \tag{37}$$

Suppose that W has been subjected to the hydrodynamic normalization at infinity. Multiplying both sides by z and sending z to infinity results in the following expression for the halfplane capacity of W:

$$c = \frac{1}{\pi} \int_{-\infty}^{\infty} Im\ W^{-1}(t) dt. \tag{38}$$

This can also be thought of as integrating over a loop around the region where W^{-1} is not analytic. This would give us the residue[10] of W^{-1}, which consequentially is $-c$.

---

[10]The residue at a pole is defined as the coefficient of the $1/z$ term in the Laurent series of W^{-1} expanded around the given pole.

9.1 The Dirac delta function

Conceptually we can think of the Dirac delta function as being an impulse which lasts for an infinitesimally small amount of time, like the force created when you strike a hammer against another object. Since we have a finite amount of 'force' compressed to an infinitely small area, it follows that the generating function must be infinite. On a similar note, we do not want our generating function to be too large other wise the 'force' will no longer be finite (i.e. we would not be able to stop the hammer after we swung it). In order to construct such a function we require that the area between the x-axis and the function be 1. Suppose we want the 'force' to be felt at the point x'. Let δ_1 be the step function of width Δx_1, height $1/\Delta x_1$ and centered at x' as in figure 18.
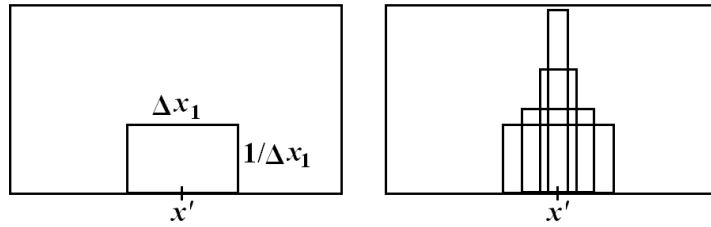

Figure 18: The figure on the left illustrates the step function δ_1. On the right are the δ_n's as $\Delta x_n \to 0$. The area under the δ_n functions remains unitary.

Now construct the functions δ_n with width Δx_n, height $1/\Delta x_n$ and centered at x' such that $\Delta x_n > \Delta x_{n-1}$. Taking the limit as $\Delta x_n \to 0$ gives a normalized function that is zero on the whole real line and has a spike at the point x'.[11] A function exhibiting these properties is called the Dirac delta function centered at the point x' and is denoted $\delta(x - x')$.

Now suppose we have a function f defined on the whole line. If we look at $\int f(x)\delta(x - x')dx$ then the integrand is zero except arbitrarily close to x'. However, if we only look at that infinitesimal interval of f surrounding x' then f would appear to be constant there. Now we have: $\int f(x)\delta(x - x')dx \approx f(x') \int \delta(x - x')dx = f(x')$ because the area under $\delta(x - x')$ is unitary. So under integration, the Dirac delta function picks out the point at which it is centered.

References

[1] Author unavailable, *Compact Space*-Absolute Astronomy Reference,
    http://www.absoluteastronomy.com/encyclopedia/c/co/compact_space.htm.

---

[11]This is not meant to be a rigorous construction of the Dirac delta function, it is only meant to serve as a guide to understand its properties.

[2] Author unavailable, *Quasiconformal Mapping*-PlanetMath,
   http://planetmath.org/encyclopedia/QuasiconformalMapping.html.

[3] W. Boyce, R. DiPrima, *Elementary Differential Equations and Boundary Value Problems*-
   John Wiley and Sons, Inc., Hoboken, New Jersey, 2005.

[4] S. Fisher, *Complex Variables: Secand Edition*-Dover Publication, Inc., Mineola, 1990, 224-
   241.

[5] G. Folland, *Advanced Calculus*-Prentice Hall, Upper Saddle River, New Jersey, 2002, 30-32.

[6] I. Gruzberg, L. Kadanoff, *The Loewner Equation: Maps and Shapes*-Journal of Statistical
   Physics, Vol. 114, Nos. 516, March 2004.

[7] L. Kadanoff, W. Kager, and B. Nienhuis, *Exact Solutions for Loewner Evolutions -*
   arXiv:math-ph/0309006.

[8] W. Kager, B. Nienhuis, *A Guide to Stochastic Lowner Evolution and its Applications*, Jour-
   nal of Statistical Physics.

[9] J. Lind, *A Sharp Condition For The Loewner Equation To Generate Slits*- Preprint, 2005.

[10] J. Lind, *Some notes on the Loewner equation in the halfplane*-(private communication).

[11] The MacTutor History of Mathematics Archive,
   http://www-history.mcs.st-andrews.ac.uk/Mathematicians/Loewner.html

[12] D. Marshall, S. Rohde, *The Loewner Differential Equation and Slit Mappings*-
   http://www.math.washington.edu/m̃arshall/preprints/loewner/loewner9.pdf.

[13] S. Rohde, O. Schramm, *Basic Properties of SLE*-arXiv:math.PR/0106036.

[14] E. Weisstein, *Homeomorphism*-MathWorld–A Wolfram Web Resource,
   http://mathworld.wolfram.com/Homeomorphism.html.

[15] E. Weisstein, *Metric Space*-MathWorld–A Wolfram Web Resource,
   http://mathworld.wolfram.com/MetricSpace.html.